Journal of Advanced Laboratory Research in Biology
E-ISSN: 0976-7614
Volume 7, Issue 1, 2016
PP 27-35
https://e-journal.sospublication.co.in

Research Article

Ultra-differentiation of Sperm Tail of Lesser Egyptian Jerboa, *Jaculus jaculus* (Family: Dipodidae)

Osama M. Sarhan[1,3*] and Hany A. Hefny[2,4]

[1]*Department of Zoology, Faculty of Science, Fayoum University, Egypt.*
[2]*Department of Zoology, Faculty of Science, Suez Canal University, Egypt.*
[3]*Department of Biology, Faculty of Applied Science, Umm Al-Qura University, KSA.*
[4]*Department of Biology, University College, Um Al Qura University Al-Jomoum KSA.*

Abstract: In the present study, events of sperm tail differentiation in Lesser Egyptian Jerboa, *Jaculus jaculus* were studied for the first time. Generally, stages of sperm tail differentiation are more or less similar to that described by other studies in other rodents. In the present species, special structures were observed. These structures include, first: the formation of a hollow large unit of microtubules that appears to surround the nuclear envelope at its equatorial plane. The manchette microtubules (MMs) are re-oriented toward the longitudinal direction and attached along hollow large unit of microtubules. Second, the formation of perinuclear space filled with an electron-translucent substance surrounds the posterior third of the developing nucleus. Third, the nuclear fossa and the connecting piece were inserted in the ventrodorsal region of the nucleus. Fourth, the fibrous sheath (FS) is formed of dextral spiral fibrous ribs. Finally, the sperm tail of the present species has a single outer FS, however, other rodents, having additional inner fibrous units, between the outer FS and the inner developing axoneme.

Keywords: Ultrastructure, Sperm tail, Lesser Egyptian Jerboa, *Jaculus jaculus*, Rodents, Mammals.

1. Introduction

Although Lesser Egyptian Jerboa, *J. jaculus* has a wide geographical range in the middle-east with diverse habitats, including coastal sand dunes, desert, semi-desert and rocky regions, it is recorded in the red list of threatened species [1]. In Egyptian mammals, insufficient data have published to explain the stages of spermiogenesis in the mammalian fauna of Egypt. Shahin and Ibraheem [2] described two morphs of spermatozoa in Egyptian dipodids. The sperm head has long paddle-shaped of pear-short heads with long or short tails, however, their connecting pieces may be inserted centrally or attaches mid basally to the lower concavity at the base of the sperm head. However, the stages of spermiogenesis of the Egyptian jerboas including present species was not investigated in details. Furthermore, Sarhan [3] studied spermiogenesis of Egyptian fat-tailed gerbil, *Pachyuromys duprasi*. He described very long acrosomal segment that capping the entire nucleus, with unique structures including special mitochondrial sheath (MS), two FS and fin-like structure supported by dorsal and ventral pairs of fibrous masses that disappear in the same structure of the end piece.

Spermiogenesis involves highly regulated developmental and morphological stages during which quiescent, inactive spermatids gain new movable shapes with highly specialized heads, necks, middle pieces, in addition, principal and end pieces of the tail regions [3] with disposal of excess cytoplasmic components [4]. Mammalian sperm head and tail differentiation has been studied in the platypus, *Ornithorhynchus anatinus* [5], shrews [6-8], bats, *Rhinopoma kinneari* and *Myotis macrodactylus* [9-10], marsupials [11,12], cats [13], as well as in primates, such as *Callithrix jacchus* and *Rhesus monkey* [14,16], and man [17-19]. However, spermiogenesis of rodents [20-22] was also studied in mice [23-25], rat [26,27], and Guinea pig [28,29].

Stages of sperm tail differentiation include the formation of specific structures in the neck's connecting piece, formation of axial filament, MS and FS in the middle piece that terminates at the annulus, in addition, study the fine structure of the principal and a terminal end piece of the tail [30-36]. These published data of mammalian spermiogenesis described numerous fine structures which are specific to different species, but none, dealing with Lesser Egyptian Jerboa. Thus, the present study aimed to discover the specific ultra-

*Corresponding author:
E-mail: sarhanomm5975@gmail.com.

structures of sperm tail differentiation of the present threatened species, *J. jaculus*.

2. Material and Methods

2.1. Animals

Ten adult males of Lesser Egyptian Jerboa, *J. jaculus* were collected, during the period of their sexual activity between April and May, from the Marsa Matrouh region, at the northwest coast of Egypt.

2.2. Dissection and preparation of tissues

Animals were dissected, their testes extracted, immediately washed in cold cacodylate buffer, cut into thin slices and fixed for 6h using 2.5% glutaraldehyde in 0.1mol cacodylate buffer adjusted at 7.2 pH. One hour later, selected sliced were cut into 1mm units for good fixation, washed in fresh cacodylate buffer to remove residual tissues and transferred into small brown bottles filled with fresh 2.5% cold glutaraldehyde to complete fixation in the refrigerator. After fixation, the small specimens washed in cacodylate buffer and post-fixed for 3 hours by adding 1% cold osmium tetroxide (OsO_4) dissolved in cacodylate buffer and re-washed in cacodylate buffer. Tissues were dehydrated in ascending grades of ethanol, cleared in propylene oxide and embedded in Epon-Araldite mixture. Semi-thin sections were cut at 1µm thick using glass knives, stained with toluidine blue and examined under research light microscope (Axioskop 2 Plus, Zeiss, Germany) to select the most active sites containing different stages of spermiogenesis. Ultra-thin sections were cut, stained with 1.5% aqueous uranyl acetate followed by Reynold's lead citrate and studied under a Jeol "JEM-1200 EXII" operating at 60-70kv. Selected figures were taken for description.

3. Results

Early spermatids of Lesser Egyptian Jerboa, *J. jaculus* have spherical nucleus with fine chromatin granules and their cytoplasm showed few mitochondria. In addition, numerous solitary microtubules arranged under the plasma membrane, and around the nuclear envelope that oriented in circular patterns (Fig. 1). Briefly, the events of the present sperm tail differentiation include nuclear elongation, that protrudes into anterior and posterior directions (PN) (Figs. 2, 3), formation of a basal plate (BP), and nuclear fossa (NF), at its posterior ventrodorsal side (Figs. 2, 3). The situation of this fossa shows that the connecting piece of the tail is attached to the sperm head at this unexpected situation (Figs. 2, 3). Moreover, the proximal (PC) and distal (DC) centrioles are fitted in or nearby the nuclear fossa (NF) (Figs. 2, 3, 5), and the cytoplasmic components are aggregated at the posterior end of the sperm head, namely connecting piece (CP) which mainly supported by longitudinal bundles of "MMs" (Figs. 3-9). Finally, unique FS and axial filament are formed (Figs. 12-19). Thus, the developing spermatid consists of a head with an elongated nucleus capped with different adjacent, abutted segments of acrosome connecting piece and middle piece (Fig. 6 & 9).

With more detail, Figures 10-12 show specific structures in the neck and middle piece of the sperm. In the neck region, the connecting piece of the tail shows the insertion of proximal and distal centrioles in the NF, which situated at the ventrodorsal side of the nucleus. Also, the neck region contains centrioles, chromatoid bodies (CB), skeleton of the connecting piece, which, represented by longitudinal bundles of MMs (Figs. 3, 6 & 9). The mechanism of microtubules re-orientation starts at equatorial level of the nuclear envelope, whereas, some microtubules unite together to form large hollow microtubule unit (MtU) running in a circular pathway (Figs. 6 & 8). At this point, the acrosomal cap stop, however, other longitudinal bundles of microtubules (Figs. 2-4) attach to the circular MtU (Figs. 6-9). MMs draw the cell membrane to surround both acrosomal cap and nuclear envelope, in the same time, forcing other cytoplasmic components towards connecting piece of the tail (Figs. 4-9). Also, a new cavity, filled with translucent material, appears to surround the posterior nuclear protrusion as a resistance structure, which may be protects the chromatin during the condensation period. Figs. from 4 to 9 showed posterior perinuclear space, which gradually increases to surround the posterior nuclear protrusion (PN). It is worth to mention that this space is located between anterior (ANS) and posterior nuclear shelves (PNS) as shown in Figure 9.

The middle piece involves a growing axoneme (AX) surrounded by ribs of a unique fibrous sheath (RFS). The outstanding rear forms of FS, which is represented by contiguous fibrous ribs that arranged in a dextral spiral (Fig. 11). Figures 13 and 14 show mitochondria surround the axial filament in the transverse sections in the different parts of the middle piece including the initial (IMP), posterior (PMP) and terminal (TMP) portions. The terminal end of the middle piece is restricted by an annulus (AN) formed of a poor and thin discoid fibrous plate (Fig. 15) that allows the growing axoneme and the surrounding FS to protrude and extends posteriorly, forming a long principal piece and a thick short end piece. In both regions, a relatively thick FS surrounds an axial filament. Figures 16-19 show that the ultra-structures of the principal and the end piece of the sperm tail are more or less similar in its structure and diameter of the FS. In the principal piece, the FS has homogeneous fibrous ribs, with two large ribs, situated at its lateral sides (LFR) (Fig. 16). The transverse sections showed the structure of FS and axial filament, narrowing towards the end of the tail with thinner fibrous ribs and constant radius of the axial filament (Figs. 17-19).

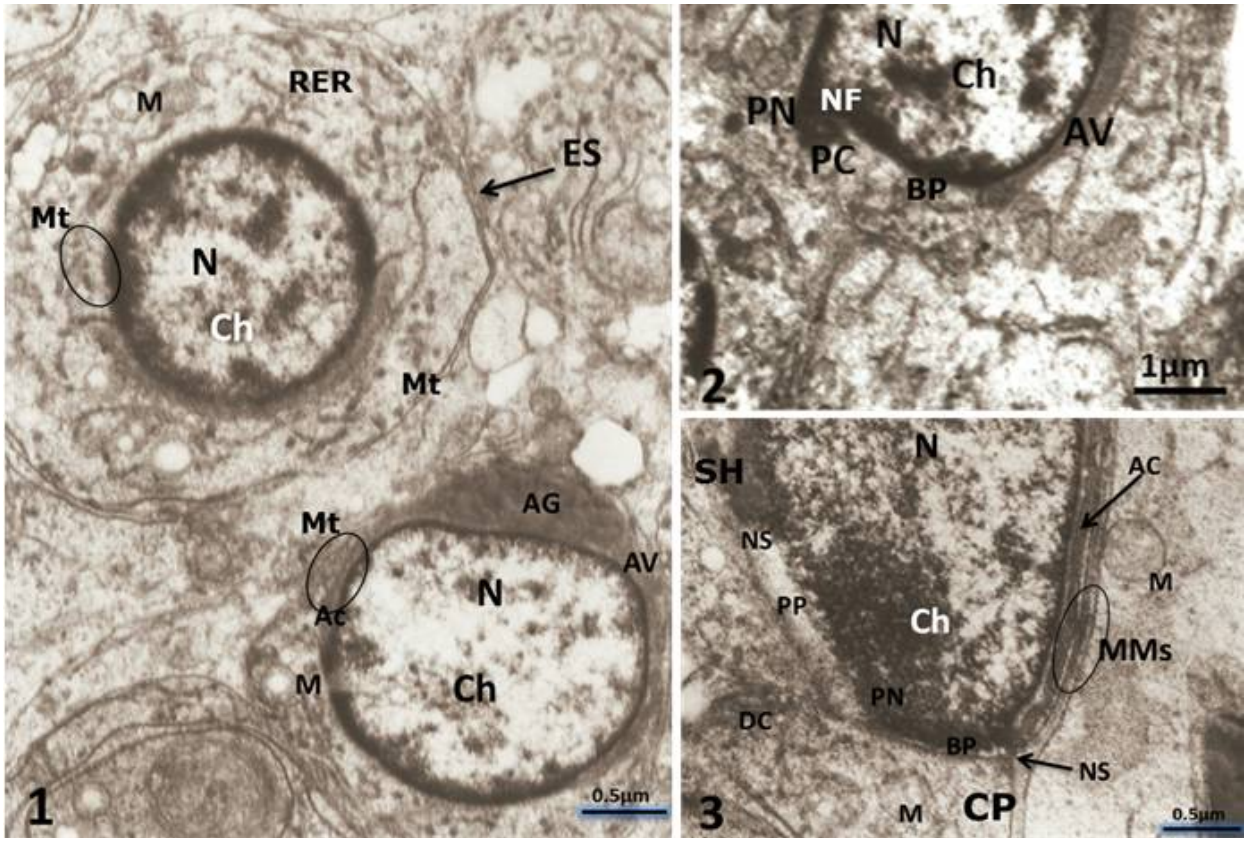

Fig. 1. Electron Micrographs showed two early spermatids. Upper: early spermatid (ES) with round nucleus (N), fine chromatin granules, and some mitochondria (M) can be seen. Lower spermatid showed formation of large triangular acrosomal granule (AG), acrosomal vesicle (AV) formed of a dark band surround the upper half of the nucleus as acrosomal cap (AC). Bar 0.5µm. **Fig. 2.** Electron Micrograph showed the next stage where the posterior ventrodorsal end of the nucleus protrudes (PN) to form curved fold that surrounds the proximal centriole (PC). Note that the first sign of tail formation is depositing centrioles at the posterior end of the nucleus and accumulation of mitochondria (M) behind the nucleus. Bar 1µm. **Fig. 3.** Electron Micrograph showed the posterior portion of the nucleus at the stage of chromatin condensation. The microtubules surround the growing acrosomal cap (AC) that ends at the nuclear shelf (NS) and reoriented to the longitudinal direction. Note that the presences of a thick basal plate at the posterior nuclear protrusion (PN), in addition, the presence of distal centriole at the posterior ventrolateral side of the nucleus (DC). Bar 1µm.

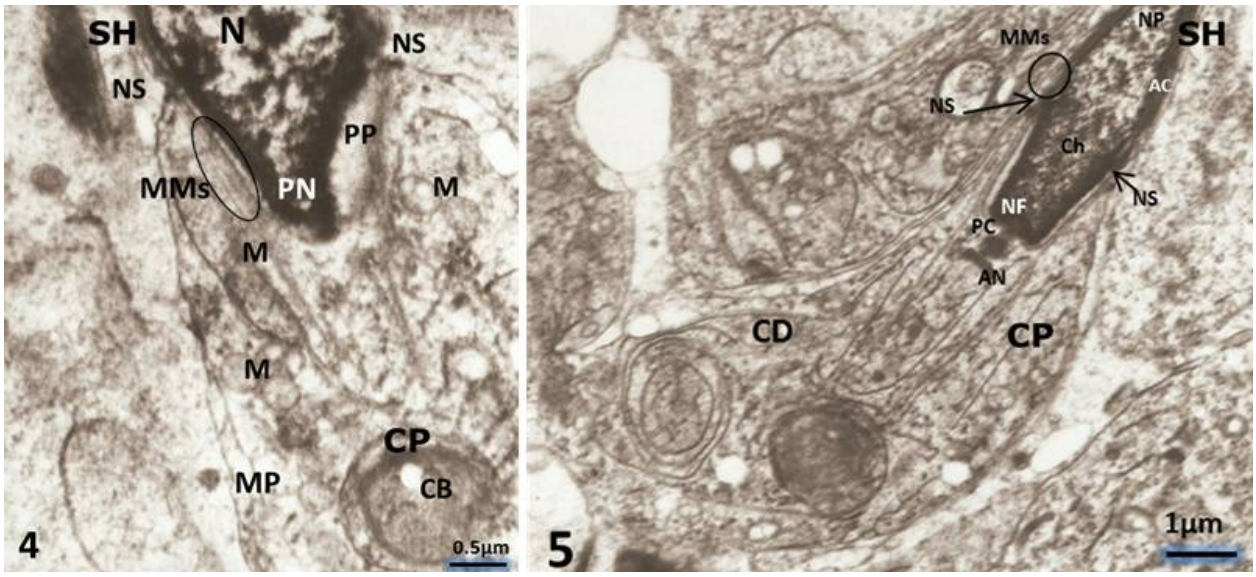

Fig. 4. Electron Micrograph showed increased the nuclear protrusion (PN) downward, presence of posterior perinuclear space (PP), longitudinal bundles of MMs, the middle piece and the presence of large dark mass known as chromatoid body. Bar 0.5µm. **Fig. 5.** Electron Micrograph showed invagination of the basal plate into nuclear fossa that lodge the proximal centriole (PC), formation of dense plate known as annulus (AN), and accumulation of numerous vesicles in a cytoplasmic droplet (CD). Bar 1µm.

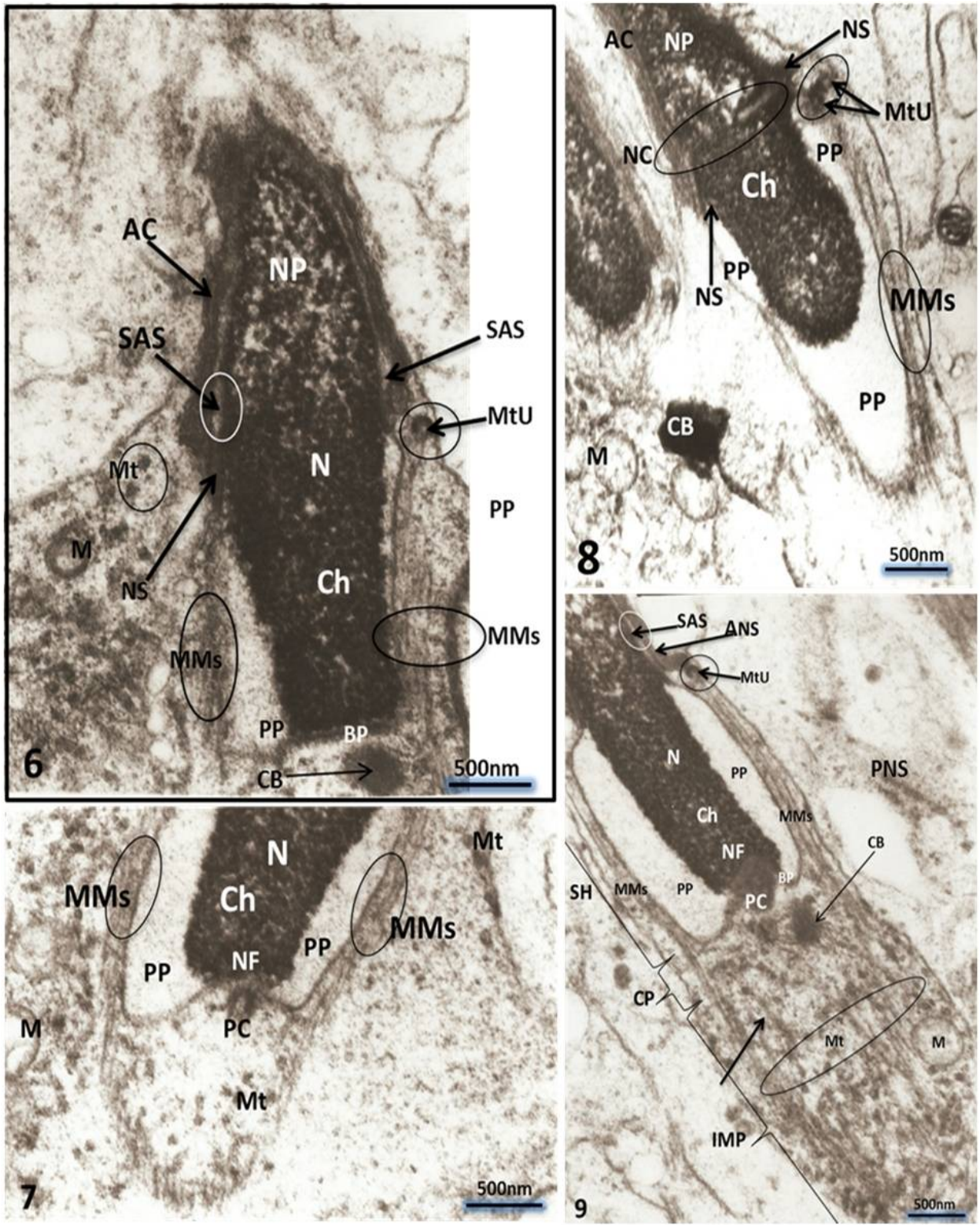

Fig. 6. Electron Micrograph showed the nucleus of developing spermatid at stage of nuclear condensation. Note that the posterior half of the nuclear envelope illustrated the resting point of acrosomal cap at the nuclear shelf. At this level, a union of several microtubules occurs to form single or double large hollow units (MtU) that support longitudinal MMs which support the head with the neck, middle and principal pieces of the sperm tail. Mt: solitary microtubule units that orient in a circular pattern, PP: Posterior perinuclear space. Bar 500nm. **Figs. 7-9.** Electron Micrographs showed stages of re-orientation of circular microtubule (Mt) (Fig. 7) to the longitudinal pathway (Figs. 8 & 9). The role of longitudinal MMs are to support the tight connection between sperm head (SH), connecting piece (CP) and the initial segment of the sperm middle piece (IMP). PP: proximal centriole is situated in the nuclear fossa (NF), PP: Posterior perinuclear space (PP). Bars showed magnifications for each figure.

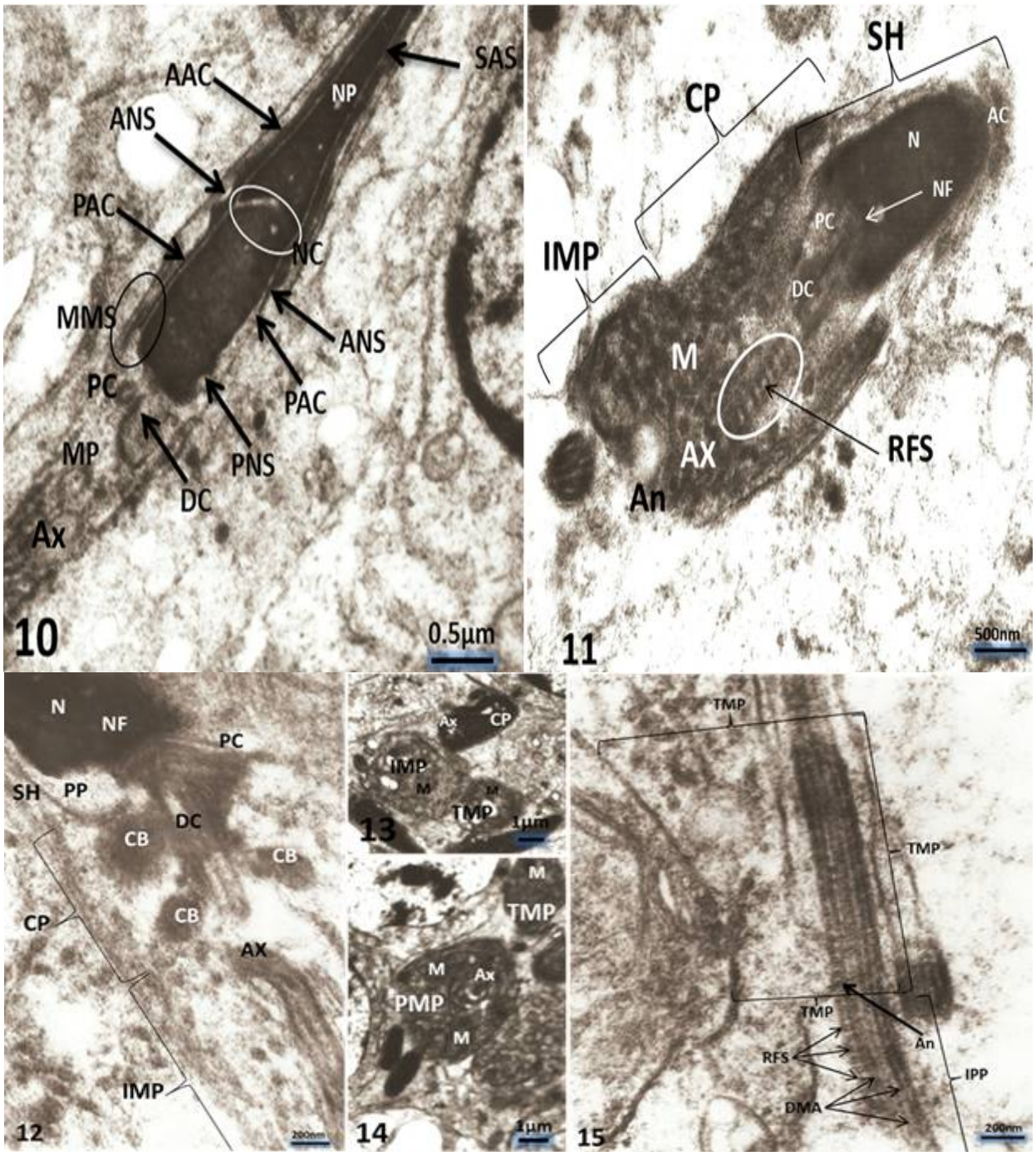

Fig. 10. Electron Micrograph showed the posterior part of the nucleus after complete chromatin condensation and a tight connection between sperm head and connecting piece in the neck region of developing spermatozoon. Bar 0.5µm. **Fig. 11.** Electron Micrograph showed different parts of nearly developed spermatozoon. Note that the sperm head (SH) is attached to the initial segment of the sperm middle piece by differentiated connecting piece (CP). The proximal centriole (PC) is situated in the nuclear fossa (NF); the distal centriole (DC) is oriented longitudinally, where the axoneme is growing. In turn, it is supported by a unique FS that formed a ring of contiguous fibrous ribs (RFS) that arranged in dextral spiral. Note that numerous mitochondria are accumulated in the initial segment around the axial filament (AX) in the middle piece (IMP). Bar 500nm. **Fig. 12**. Electron Micrograph showed the connecting piece (CP) at the posterior region of sperm head (SH). The connecting piece contains a distal centriole, which is situated perpendicular with the proximal one. Note the formation of the axial filament. Bar 200nm. **Figs. 13 & 14.** Electron Micrograph showed transverse sections through the connecting piece (CP), initial segment of the middle piece (IMP), and the terminal portion of the middle piece (TMP). AX: axial filament, M: mitochondria. Bar 1µm. **Fig. 15.** Electron Micrograph showed a longitudinal section through the terminal portion of the middle piece (TMP), that end at the annulus, and the initial portion of the tail principal piece (IPP). Note that the axial filament is surrounded by ribs of FS, and supported by peripheral doublets of microtubules, in addition to a central pair (DMA).

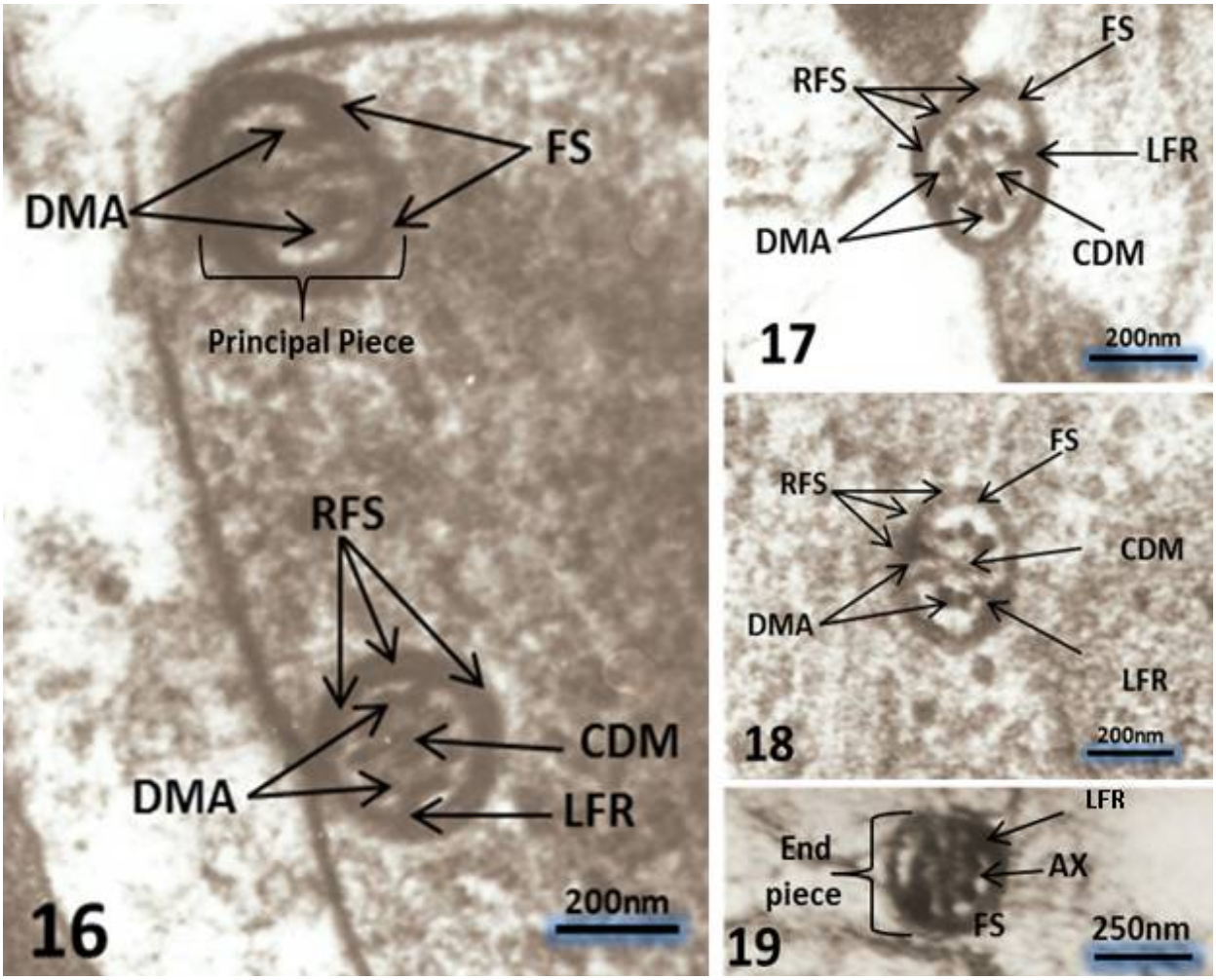

Figs. 16 & 17. Electron Micrograph showed a transverse section through a principal piece of sperm. Note that the axial filament is surrounded by thick ribs of FS. Note that these ribs form of similar fibrous masses except two lateral large fibrous masses that are run toward the terminal end of tail (LFR). **Figs. 18 & 19**. Electron Micrograph showed a transverse section through the end piece of the sperm tail. Note that the FS becomes thinner. Although, the sperm tail is long but it is still surrounded by an FS with enlarged two large lateral fibrous masses.

4. Discussion

The present results showed that the sperm has a relatively long head, neck with a connecting piece inserted in the posterior ventrodorsal side of the nucleus and the middle piece of medium size, in addition to the tail of medium length. Shahin and Ibraheem [2] described paddle-shaped long head with long tail in smaller jerboa, *Allactaga tetradactyla*, while pear-shaped short heads with short tails in both lesser and greater Egyptian jerboa. The sperm head of later species have symmetrical bilateral flattened shape, without any hooks or processes, and capped by a massive symmetrical apical acrosomal segment. The connecting piece was posteriorly inserted off-centre at the base of the sperm head or mid basally to the lower concave surface of the sperm head. Moreover, very long tail regions were reported in fat-tailed gerbil Sarhan [3].

The present results proved that the MMs play an essential role in sperm tail differentiation, especially the posterior nuclear protrusion, formation of the NF, supporting the attachment between the sperm head and the connecting piece of the tail and formation of the doublet microtubules of the axial filaments. Also, Wang and Sperry [4] considered that MMs are basic and essential units for the developing germ cells. Reorientation of solitary microtubules into longitudinal direction was also described by numerous investigators in bats [10], mice [4, 37] and in fat-tailed gerbil [3]. While in marsupials, Lin [4] described that MMs were oriented in both longitudinal and circular directions. As regards to their function, the present authors suggest that the MMs play multifunctional missions, including the nuclear elongation, formation of NF, supporting the attachment between sperm head and the connecting piece of the tail, in addition, transportation of ATP, as a source of energy, produced by mitochondrial units in the middle piece to the distal end of the tail. Also, it was reported that MMs play an important role in the nuclear elongation and may facilitate the transportation of material between the nucleus and cytoplasm [22,38].

However, it acts as a track for the transport of cellular component not only between the nucleus and cytoplasm but also from the apical to the distal end of the elongating spermatid [39,40]. On the other hand, the formation of a hollow large microtubule unit, that runs in a circular direction at the equatorial level of the nucleus, was not described before. This novel unit works as holding axis extends to surround the equatorial plane of the nucleus in which microtubule run longitudinally inducing pressure on the perinuclear space for nuclear prolongation at the same time to protect chromatin during this period. The function suggested by the present authors was not discussed before. The NF described in the present species was reported in the posterior end of the nuclei of different mammalian spermatozoa. The present fossa is situated in the ventrodorsal aspect of the nucleus. The NF has described also, in human spermatids [19], and in the shrews [8]. It is also confirmed in some Egyptian gerbils, in a central and or mid-basal portion of the nucleus [2]. In addition, this fossa was reported at the posterior end of the nucleus as described for other different mammalian spermatozoa [3, 5, 8]. However, in other Egyptian gerbils, it is situated in the central and/or mid-basal portion of the nucleus [2, 3].

The ultrastructure of *J. jaculus* sperm tail shows it is divided into four major parts, namely: neck piece, midpiece, principal piece and a terminal end-piece. These major parts are in agreement with those described by many authors [40, 41]. These major parts were further subdivided into anterior and posterior subdivisions [3].

The neck region of the sperm tail connects between the NF and the midpiece. It consists of the CBs, connecting piece, which surrounds the proximal and distal centrioles. These findings agree with described in other rodents [2, 3, 20, 21, 24]. The present work suggests that the "CB" has an essential role concerned with the formation of some cytoskeletal structures in the tail flagellum such as the connecting piece and FS. Some investigators reported that it contains ribonucleoproteins, mRNA, mRNA-binding proteins and some proteins necessary for the late spermiogenesis [31]. Other research workers declared that CBs might be served as nucleoproteins degradation center [33].

The midpiece begins at the neck piece and contains MS, FS, and axoneme. It terminates down the sperm flagellum at the annulus, which marks the beginning of the principal piece [35]. In the present study, the annulus is a thin discoid plate at the end of the midpiece. It allows the growing axoneme to stretch and shuttles through it; therefore the mitochondria cannot leave the midpiece. The annulus was described in all mammalian spermatozoa [3, 8, 35].

As regards to the MS, the mitochondria are distributed as a loose MS pattern. The MS was described also in the midpiece in human sperm tail [19] as well as in the marmoset monkey, bat and Korean shrews [10, 8].

The axoneme originates at the distal centriole and extends throughout the length of the flagellum. The initial segment of the principal piece consists of an axial filament surrounded by a ring of FS. However, two FS layers were reported in fat-tailed gerbil [3].

The perinuclear space observed in the present study was not described and discussed before.

5. Conclusion

From these results, it could be concluded that the ultrastructure of sperm tail of Lesser Egyptian Jerboa, *J. jaculus* is to some extent similar to that described in other rodents. Worth mentioning is that the first report showing special structures in the sperm tail such as formation of a hollow large unit of microtubules, surrounding the nuclear envelope at its equatorial plane. The MMs are re-oriented to the longitudinal direction and attached along hollow large unit of microtubules; formation of perinuclear space at the posterior third of the developing nucleus; the location of nuclear fossa and the insertion of the connecting piece were observed in the ventrodorsal region of the nucleus. In addition, Spiral ribs of dextral direction of the FS were observed. Finally, the sperm tail of the present species has a single outer FS in comparison with that described in other rodents that having additional inner fibrous units.

References

[1]. IUCN (International Union for Conservation of Nature, 2015). *Jaculus jaculus*. In: IUCN 2015. The IUCN Red List of Threatened Species. Version 2015.2. http://www.iucnredlist.org. Downloaded on 14 July 2015.

[2]. Shahin, A.A.B. and Ibraheem, M.H. (1998). Sperm morphology of the dipodid rodents (Jerboas) common in Egypt. *Belgian Journal of Zoology*, 128(2): 189-200.

[3]. Sarhan, O.M.M. (2009). Spermiogenesis of Egyptian mammals: 1-Sperm head and tail differentiation of fat-tailed gerbil, *Pachyuromys duprasi*. *Egypt. J. Zool.*, 53: 283-309.

[4]. Wang, R. and Sperry, A.O. (2008). Identification of a novel leucine-rich repeat protein and candidate PP1 regulatory subunit expressed in developing spermatids. "Electronic version". *BMC Cell Biology*, 9:9 doi:10.1186/1471-2121-9-9.

[5]. Lin, M. and Jones, R.C. (2000). Spermiogenesis and spermiation in a monotreme mammal, the platypus, *Ornithorhynchus anatinus*. *Journal of Anatomy*, 196(2): 217-232.

[6]. Mori, T., Arai, S., Shiraishi, S. and Uchida, T.A. (1991). Ultrastructural Observations on Spermatozoa of the Soricidae, with Special Attention to a Subfamily Revision of the Japanese Water Shrew *Chimarrogale himalayica*. *J. Mamm. Soc. Japan*, 16: 1-12.

[7]. Jeong, S.J., Yoo, J.Y. and Jeong, M.J. (2004). Ultrastructure of the Abnormal Head of the Epididymal Spermatozoa in the Big White-Toothed Shrew, *Crocidura lasiura*. *Korean Journal of Electron Microscopy*, 34(3): 179-184.

[8]. Jeong, S.J., Park, J.C., Kim, H.J., Bae, C.S., Yoon, M.H., Lim, D.S., Jeong, M.J. (2006). Comparative fine structure of the epididymal spermatozoa from three Korean shrews with considerations on their phylogenetic relationships. *Biocell*, 30(2): 279-286.

[9]. Singwi, M.S. and Lall, S.B. (1983). Spermatogenesis in the non-scrotal bat *Rhinopoma kinneari* Wroughton (Microchiroptera: Mammalia). *Acta Anat. (Basel)*, 116(2): 136-145.

[10]. Jung-Hun, L. (2003). Cell Differentiation and Ultrastructure of the Seminiferous Epithelium in *Myotis macrodactylus*. *Korean Journal of Electron Microscopy*, 33(1): 25-39.

[11]. Sapsford, C.S., Rae, C.A. and Cleland, K.W. (1969). Ultrastructural studies on maturing spermatids and on Sertoli cells in the bandicoot *Perameles nasuta* Geoffroy (Marsupialia). *Aust. J. Zool*., 17: 195-292.

[12]. Ricci, M. and Breed, W.G. (2005). Morphogenesis of the fibrous sheath in the marsupial spermatozoon. *J. Anat.*, 207(2): 155-164.

[13]. Burgos, M.H. and Fawcett, D.W. (1955). Studies on the fine structure of the mammalian testis. I. Differentiation of the spermatids in the cat (*Felis domestica*). *J. Biophys. Biochem. Cytol.*, 1(4): 287-300.

[14]. Holt, W.V. and Moore, H.D.M. (1984). Ultrastructural aspects of spermatogenesis in the common marmoset (*Callithrix jacchus*). J. Anat., 138: 175-188.

[15]. Moreno, R.D., Ramalho-Santos, J., Chan, E.K., Wessel, G.M. and Schatten, G. (2000a). The Golgi apparatus segregates from the lysosomal/acrosomal vesicle during rhesus spermiogenesis: structural alterations. *Dev. BioI.*, 219: 334-349.

[16]. Moreno, R.D., Ramalho-Santos, J., Sutovsky, P., Chan, E.K. and Schatten, G. (2000b). Vesicular traffic and Golgi apparatus dynamics during mammalian spermatogenesis: Implications for acrosome architecture. *Biol. Reprod.*, 63: 89-98.

[17]. Dadoune, J.P. and Alfonsi, M.F. (1986). Ultrastructural and cytochemical changes of the head components of human spermatids and spermatozoa. *Gamete Res.*, 14: 33-46.

[18]. Kim, Y.H., de Krester, D.M., Temple-Smith, P.D., Hearn, M.T. and McFarlane, J.R. (1997). Isolation and characterization of human and rabbit sperm tail fibrous sheath. *Mol. Hum. Reprod.*, 3(4): 307-313.

[19]. Toyama, Y., Iwamoto, T., Yajima, M., Baba, K. and Yuasa, S. (2000). Decapitated and decaudated spermatozoa in man, and pathogenesis based on the ultrastructure. *Int. J. Androl.*, 23(2): 109-115.

[20]. Challice, C.E. (1953). Electron microscope studies of spermiogenesis in some rodents. *J. R. Microsc. Soc.*, 73: 115-127.

[21]. Rattner, J.B. and Brinkley, B.R. (1972). Ultrastructure of mammalian spermiogenesis. 3. The organization and morphogenesis of the manchette during rodent spermiogenesis. *J. Ultrastruct. Res.*, 41(3):209-18.

[22]. Russell, L.D., Russell, J.A., MacGregor, G.R. and Meistrich, M.L. (1991). Linkage of manchette microtubules to the nuclear envelope and observations of the role of the manchette in nuclear shaping during spermiogenesis in rodents. *Am. J. Anal.*, 192: 97-120.

[23]. Gardner, P.J. (1966). Fine structure of the seminiferous tubule of the Swiss mouse. The spermatid. *Anat. Rec.*, 155: 235-249.

[24]. Jin, Q.S., Kamata, M., Garcia del Saz, E. and Seguchi, H. (1995). Ultracytochemical study of trimetaphosphatase activity during acrosomal formation in the mouse testis. *Histol. Histopathol.*, 10: 681-689.

[25]. Ho, H.C., Tang, C.Y. and Suarez, S.S. (1999). Three-dimensional structure of the Golgi apparatus in mouse spermatids: a scanning electron microscopic study. *Anat. Rec.*, 256: 189-194.

[26]. Minamino, T. (1955). Spermiogenesis in the albino rat as revealed by electron microscopy. *Electron Microsc*., 4: 249-253.

[27]. Tang, X.M., Lalli, M.F. and Clermont, Y. (1982). A cytochemical study of the Golgi apparatus of the spermatid during spermiogenesis in the rat. *Am. J. Anat.*, 163: 283-294.

[28]. Pelletier, R.M. and Friend, D.S. (1983). Development of membrane differentiations in the guinea pig spermatid during spermiogenesis. *Am. J. Anat.*, 167: 119-141.

[29]. Burgos, M.H. and Gutierrez, L.S. (1986). The Golgi complex of the early spermatid in guinea pig. *Anat. Rec.*, 216: 139-145.

[30]. Sapsford, C.S., Rae, C.A. and Cleland, K.W. (1970). Ultrastructural studies on the development and form of the principal piece sheath of the bandicoot spermatozoon. *Aust. J. Zool.*, 18: 21-48.

[31]. Oko, R. and Clermont, Y. (1989). Light microscopic immunocytochemical study of fibrous sheath and outer dense fiber formation in the rat spermatid. *Anat Rec*., 225: 46-55.

[32]. Rawe, V.Y., Galaverna, G.D., Acosta, A.A., Olmedo, S.B., Chemes, H.E. (2001). Incidence of tail structure distortions associated with dysplasia of the fibrous sheath in human spermatozoa. *Human Reproduction*, 16(5): 879-886.

[33]. Yokota, S. (2008). Historical survey on chromatoid body research. *Acta Histochem. Cytochem.*, 41(4): 65-82.

[34]. Guan, J., Kinoshita, M. and Yuan, L. (2009). Spatiotemporal Association of DNAJB13 with the annulus during mouse sperm flagellum development. *BMC Dev. Biol.*, 9: 23. doi: 10.1186/1471-213X-9-23.

[35]. Lim, S.L., Qu, Z.P., Kortschak, R.D., Lawrence, D.M., Geoghegan, J., Hempfling, A.L., Bergmann, M., Goodnow, C.C., Ormandy, C.J., Wong, L., Mann, J., Scott, H.S., Jamsai, D., Adelson, D.L., O'Bryan, M.K. (2015). HENMT1 and piRNA Stability are Required for Adult Male Germ Cell Transposon Repression and to Define the Spermatogenic Program in the Mouse. *PLoS Genet.*, 11(10): e1005620. doi: 10.1371/journal.pgen.1005620.

[36]. Fouquet, J.P., Kann, M.L., Soues, S. and Melki, R. (2000). ARP1 in Golgi organisation and attachment of manchette microtubules to the nucleus during mammalian spermatogenesis. *J. Cell Sci.*, 113: 877-886.

[37]. Meistrich, M.L., Trostle-Weige, P.K., Russell, L.D. (1990). Abnormal manchette development in spermatids of azh/azh mutant mice. *Am. J. Anat.*, 188(1): 74-86.

[38]. Kierszenbaum, A.L. (2002). Intramanchette transport (IMT): managing the making of the spermatid head, centrosome, and tail. *Mol. Reprod. Dev.*, 63(1): 1-4.

[39]. Eddy, E.M., Toshimori, K. and O'Brien, D.A. (2003). Fibrous sheath of mammalian spermatozoa. *Microsc. Res. Tech.*, 61: 103-115.

[40]. Turner, R.M. (2003). Tales from the Tail: What do we really know about sperm motility? *J. Androl.*, 24(6):790-803.

Abbreviations:

AAC	Anterior acrosomal cap	FS	Fibrous sheath	PAS	Posterior acrosomal segment
Ac	Acrosomal Cap	IMP	Initial segment of middle piece	PC	Proximal centriole
AG	Acrosomal granule	IPP	Initial segment of tail principal piece	PN	Posterior nuclear protrusion
An	Annulus	LFR	Lateral fibrous rib of fibrous sheath	PMP	Posterior portion of the middle piece
ANS	Anterior nuclear shelf	M	Mitochondria	PNS	Posterior nuclear shelf
AV	Acrosomal vesicle	MMs	Manchette microtubules	PP	Posterior perinuclear space
AX	Axoneme (Axial filament)	MP	Middle piece	PrP	Principal piece
BP	Basal plate	MS	Mitochondrial sheath	PS	Enlarged perinuclear space
CB	Chromatoid body	Mt	Microtubule(s)	PSS	Posterior subacrosomal space
CD	Cytoplasmic droplet	MtU	Microtubule unit	RER	Rough endoplasmic reticulum
CDM	Central doublet microtubule of axoneme	N	Nucleus	RFS	Ribs of fibrous sheath
Ch	Chromatin	NC	Nuclear constriction	SAS	Subacrosomal space
CP	Connecting piece	Ne	Neck region of sperm tail	SC	Subacrosomal cone
DC	Distal centriole	NF	Nuclear fossa	SH	Sperm head
DMA	Doublet microtubule of axoneme	NP	Nuclear protrusion	TEP	Terminal portion of tail end piece
DEP	Distal portion of tail end piece	NS	Nuclear shelf	TMP	Terminal portion of middle piece
ES	Early spermatid	PAC	Posterior limb of acrosomal cap		